

---

# Brain-inspired sparse training enables Transformers and LLMs to perform as fully connected

---

Yingtao Zhang<sup>1,2</sup> Jialin Zhao<sup>1,2</sup> Wenjing Wu<sup>1,2</sup> Ziheng Liao<sup>1,2,3</sup> Umberto Michieli<sup>4</sup>  
Carlo Vittorio Cannistraci<sup>1,2,3</sup>

## Abstract

This study aims to enlarge our current knowledge on application of brain-inspired network science principles for training artificial neural networks (ANNs) with sparse connectivity. Dynamic sparse training (DST) can reduce the computational demands of training and inference in ANNs, but existing methods face difficulties in maintaining peak performance at high connectivity sparsity levels. The Cannistraci-Hebb training (CHT) is a brain-inspired method for growing connectivity in DST. CHT leverages a gradient-free, topology-driven link regrowth mechanism, which has shown to achieve ultra-sparse (1% connectivity or lower) advantage across various tasks compared to fully connected networks. Yet, CHT suffers two main drawbacks: (i) its time complexity is  $\mathcal{O}(N \cdot d^3)$ -  $N$  node network size,  $d$  node degree - hence it can be efficiently applied only to ultra-sparse networks. (ii) it rigidly selects top link prediction scores, which is inappropriate for the early training epochs, when the network topology presents many unreliable connections. Here, we propose a matrix multiplication GPU-friendly approximation of the CH link predictor, which reduces the computational complexity to  $\mathcal{O}(N^3)$ , enabling a fast implementation of CHT in large-scale models. Moreover, we introduce the Cannistraci-Hebb training soft rule (CHTs), which adopts a flexible strategy for sampling connections in both link removal and regrowth, balancing the exploration and exploitation of network topology. To further improve performance, we integrate CHTs with a sigmoid gradual density decay strategy, referred to as CHTss. Empirical

results show that, using 1% of connections, CHTs outperforms fully connected networks in MLP architectures on visual classification tasks, compressing some networks to less than 30% nodes. Using 5% of the connections, CHTss outperforms fully connected networks in two Transformer-based machine translation tasks. Finally, using 30% of the connections, CHTss achieves superior performance compared to other dynamic sparse training methods in language modeling (LLaMA-130M) across different sparsity levels, and it surpasses the fully connected counterpart in zero-shot evaluations.

## 1. Introduction

Artificial neural networks (ANNs) have spurred significant advancements in various fields, such as natural language processing, computer vision, and deep reinforcement learning. The most common ANNs include several fully connected (FC) layers, which represent a significant portion of parameters in recent large language models (Touvron et al., 2023a; Zhang et al., 2022). This dense connectivity poses major challenges during both the training and the deployment phases of the models. In contrast, the brain’s neural networks inherently exhibit sparse connectivity (Drachman, 2005; Walsh, 2013). This natural design in the brain leverages sparsity, suggesting a model where the number of connections does not scale quadratically with the number of neurons. This could alleviate computational constraints, enabling more scalable network architectures.

Dynamic sparse training (DST) (Mocanu et al., 2018; Jayakumar et al., 2020; Evci et al., 2020; Yuan et al., 2021; Zhang et al., 2024b) has emerged as a promising approach to reduce the computational and memory overheads of training deep neural networks while maintaining or even enhancing model performance. Unlike Pruning methods (Han et al., 2016; Frantar & Alistarh, 2023; Zhang et al., 2024a), DST starts with an already sparse initialized network and maintains this sparsity throughout the training process. Prevalent DST methods evolve the network topology during training by iteratively removing a proportion of connections and

---

<sup>1</sup>Center for Complex Network Intelligence (CCNI), Tsinghua Laboratory of Brain and Intelligence (THBI) <sup>2</sup>Department of Computer Science <sup>3</sup>Department of Biomedical Engineering, Tsinghua University, Beijing, China <sup>4</sup>University of Padova, Italy.. Correspondence to: Carlo Vittorio Cannistraci <kalokagathos.agon@gmail.com>.

regrowing an equivalent number of links.

Apart from some detailed distinctions, the primary innovation in this field centers on the development of the regrowth criterion. A notable advancement is the gradient-free regrowth method introduced by Cannistraci-Hebb training (CHT) (Zhang et al., 2024b). This method is inspired by epitopological learning—literally meaning ‘new topology’—and is rooted in brain-inspired network science theory (Cannistraci et al., 2013; Daminelli et al., 2015; Durán et al., 2017; Cannistraci, 2018; Narula, 2017). Epitopological learning explores how learning can be implemented on complex networks by changing the shape of their connectivity structure (epitopological plasticity). CHT has demonstrated remarkable advantages in training ultra-sparse ANNs with connectivity levels of 1% or lower, often outperforming fully connected networks in various tasks. However, despite these advancements, CHT encounters two major challenges: 1) During dynamic sparse training, its rigid link selection mechanism can lead to *epitopological local minima*, which severely impedes the exploration of optimal network topologies. 2) The time complexity of the CHT regrowth method, CH3-L3, is  $\mathcal{O}(N \cdot d^3)$ , where  $N$  represents the number of nodes in the network and  $d$  is the average degree. As the network becomes denser, the time complexity escalates to  $\mathcal{O}(N^4)$ , rendering it impractical for large-scale and higher density models.

In this article, we present the Cannistraci-Hebb Training soft rule (CHTs), which introduces several key innovations: 1) To address the issue of epitopological local minima, CHTs employs a multinomial distribution to sample link scores from removal and regrowth metrics, enabling more flexible and effective exploration of network topologies. 2) CHTs incorporates the novel substitution node-based link prediction mechanisms, reducing the computational time complexity to  $\mathcal{O}(N^3)$ . This improvement makes CHTs scalable to large-scale models with higher network density. 3) CHTs leverages network science principles to initialize sparse topologies for bipartite networks with small-world properties, demonstrating superior performance compared to the traditional Erdos-Renyi model. Additionally, we propose a sigmoid gradual density decay strategy, which, when integrated with CHTs, forms an enhanced framework termed CHTss. This combined approach further optimizes the training process for sparse neural networks.

To evaluate the effectiveness of the Cannistraci-Hebb Training soft rule with sigmoid density decay (CHTss), we conduct extensive experiments across multiple architectures and tasks. Firstly, to evaluate the basic concept of CHTs, we employ MLPs on benchmark datasets, including MNIST (LeCun et al., 1998), EMNIST (Cohen et al., 2017), and Fashion MNIST (Xiao et al., 2017). The results show that CHTs achieves superior performance compared to

fully connected networks with only 1% of the connections (99% sparsity) in MLPs. Further, to evaluate the end-to-end approach CHTss, we utilize Transformers (Vaswani et al., 2017) on machine translation datasets such as Multi30k en-de (Elliott et al., 2016), IWSLT14 en-de (Cettolo et al., 2014), and WMT17 en-de (Bojar et al., 2017). Additionally, we evaluate CHTss also on the LLaMA-130M model with language modeling tasks and zero-shot evaluation tasks. From the results of the above experiments, CHTss outperforms fully connected Transformers with only 5% of the links on Multi30k and IWSLT and achieves performance comparable to the fully connected LLaMA-130M in language modeling tasks on OpenWebText. Moreover, CHTss outperforms the fully connected LLaMA-130M on zero-shot evaluation tasks on GLUE (Wang et al., 2019) and SuperGLUE (Wang et al., 2020) with only 30% density. These findings underscore the potential of CHTs and CHTss in enabling highly efficient and effective large-scale sparse neural network training.

## 2. Related Work

### 2.1. Dynamic sparse training

Dynamic sparse training is a subset of sparse training methodologies. Unlike the static sparse training (also known as pruning at initialization) methods (Prabhu et al., 2018; Lee et al., 2019; Dao et al., 2022; Stewart et al., 2023), dynamic sparse training allows for the evolution of network topology during the training process. The pioneering method in this field was Sparse Evolutionary Training (SET) (Mocanu et al., 2018), which removes links based on the magnitude of their weights and regrows new links randomly. Subsequent developments have sought to refine and expand upon this concept of dynamic topological evolution. One such advancement was proposed by DeepR (Bellec et al., 2017), a method that adjusts network connections based on stochastic gradient updates combined with a Bayesian-inspired update rule. Another significant contribution is the RigL (Evci et al., 2020), which leverages the gradient information of non-existing links to guide the regrowth of new connections during training. MEST (Yuan et al., 2021) utilizes both gradient and weight magnitude information to selectively remove and randomly regrow new links, which is the same as SET. In addition, it introduces an EM&S strategy that allows the model training with a larger density and finally convergence to the desired density. The Top-KAST (Jayakumar et al., 2020) method maintains constant sparsity throughout training by selecting the top  $K$  parameters based on parameter magnitude at each training step and applying gradients to a broader subset  $B$ , where  $B \supset A$ . To avoid settling on a suboptimal sparse subset, Top-KAST also introduces an auxiliary exploration loss that encourages ongoing adaptation of the mask. Additionally, sRigL (Lasby et al.,

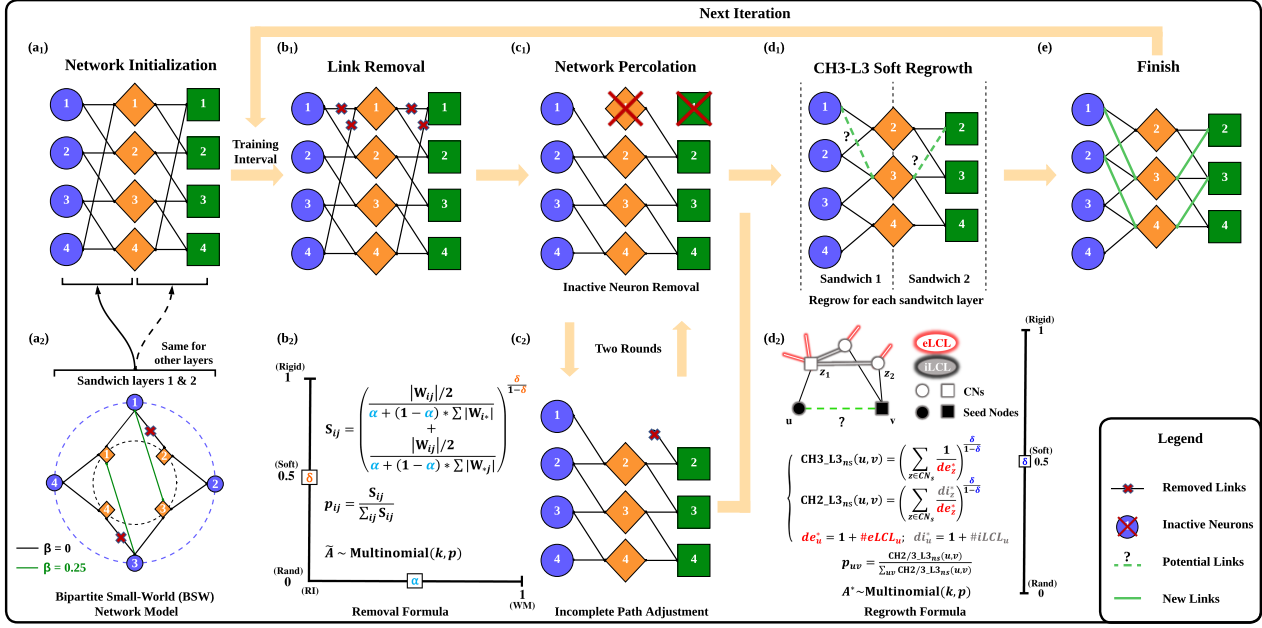


Figure 1: **Illustration of the CHTs process.** One training iteration follows the path of (a1)  $\rightarrow$  (b1)  $\rightarrow$  (c1)  $\rightarrow$  (c2)  $\rightarrow$  (d1)  $\rightarrow$  (e). (a1) Network initialization with each of the sandwich layers being a bipartite small-world (BSW) network. (a2) One sample BSW network with different  $\beta$  values (for  $\beta = 0$ , the network contains the black links; for  $\beta = 0.25$ , the network is formed by removing the marked black links and regrowing the green links). (b1) Link removal process. (b2) Formula for determining which links to remove. (c1) Removal of inactive neurons caused by link removal. (c2) Adjust and remove incomplete links caused by inactive neuron removal. (d1) Regrowth of links according to the CH2/3-L3 node-based soft rule. (d2) Detailed illustration of the CH2/3-L3 node-based soft rule. (e) Finished state of the network after one iteration. The next iteration repeats the steps (b1) - (e) from this finished state.  $\bar{A}$  indicates the removal set of the iteration and  $A^*$  is the regrown set.

2023) adapts the principles of RigL to semi-structured sparsity, facilitating the training of vision models from scratch with actual speed-ups during training phases. Despite these advancements, the state-of-the-art method remains RigL-based, yet it is not fully sparse in backpropagation, necessitating the computation of gradients for non-existing links. Addressing this limitation, Zhang et al. (Zhang et al., 2024b) propose CHT, a dynamic sparse training methodology that adopts a gradient-free regrowth strategy that relies solely on topological information (network shape intelligence), achieving an ultra-sparse configuration that surpasses fully connected networks in some tasks.

## 2.2. Cannistraci-Hebb Theory and Network Shape Intelligence

As the SOTA gradient-free link regrown method, CHT (Zhang et al., 2024b) originates from a brain-inspired network science theory. Drawn from neurobiology, Hebbian learning was introduced in 1949 (Hebb, 1949) and can be summarized in the axiom: “neurons that fire together wire together.” This could be interpreted in two ways: changing the synaptic weights (weight plasticity) and changing

the shape of synaptic connectivity (Cannistraci et al., 2013; Daminelli et al., 2015; Durán et al., 2017; Cannistraci, 2018; Narula, 2017). The latter is also called *epitopological plasticity* (Cannistraci et al., 2013) because plasticity means “to change shape,” and *epitopological* means “via a new topology.” *Epitopological Learning* (EL) (Daminelli et al., 2015; Durán et al., 2017; Cannistraci, 2018) is derived from this second interpretation of Hebbian learning and studies how to implement learning on networks by changing the shape of their connectivity structure. One way to implement EL is via link prediction, which predicts the existence and likelihood of each nonobserved link in a network. CH3-L3 is one of the best and most robust performing network automata which is inside Cannistraci-Hebb (CH) theory (Muscoloni et al., 2022) that can automatically evolve the network topology with the given structure. The rationale is that, in any complex network with local-community organization, the cohort of nodes tends to be co-activated (fire together) and to learn by forming new connections between them (wire together) because they are topologically isolated in the same local community (Muscoloni et al., 2022). This minimization of the external links induces a topological isolation of the local community, which is equivalent to forming a

barrier around the local community. The external barrier is fundamental to maintaining and reinforcing the signaling in the local community, inducing the formation of new links that participate in epitopological learning and plasticity.

### 3. Cannistraci-Hebb training soft rule with sigmoid gradual density decay

#### 3.1. Cannistraci-Hebb soft removal and regrowth

**Definition 1. Epitopological local minima.** In the context of dynamic sparse training methods, we define an epitopological local minima (ELM) as a state where the sets of removed links and regrown links exhibit a significant overlap.

Let  $A_t$  be the set of existing links in the network at the training step  $t$ . Let  $\hat{A}_t$  be the set of removal links and  $A_t^*$  be the set of regrown links. The overlap set between removed and regrown links at step  $t$  can be quantified as  $O_t = \hat{A}_t \cap A_t^*$ . An ELM occurs if the size of  $O_t$  at step  $t$  is significantly large compared to the size of  $A_t^*$ , indicating a high probability of the same links being removed and regrown repeatedly throughout the subsequent training steps. This can be formally represented as  $\frac{|O_t|}{|A_t^*|} \geq \theta$ , where  $\theta$  is a predefined threshold close to 1, indicating strong overlap. This definition is essential for the understanding of CHT, as evidenced by the article (Zhang et al., 2024b) indicating that the overlap rate between removed and regrown links becomes significantly high within just a few epochs, leading to rapid topological convergence towards the ELM. Previously, CHT implements a topological early stop strategy to avoid predicting the same links iteratively. However, it will stop the topological exploration very fast and potentially trap the model within the ELM.

In this article, we adopt a probabilistic approach where the process of regrowth can be viewed as sampling from a  $\{0, 1\}$  multinomial distribution, with the score assigned by either removal metrics or link prediction scores, introducing a "soft sampling" mechanism. In this setup, each mask value is not rigidly determined by the link prediction scores but allows for selecting (with lower probability) low-score links as new links, facilitating the escape from the epitopological local minima (ELM).

**Link removal alternating from weight magnitude and relative importance.** We illustrate the link removal part of CHTs in Figure 1b1) and b2). We employ two methods, Weight Magnitude (WM)  $|\mathbf{W}|$  and Relative Importance (RI) (Zhang et al., 2024a), to remove the connections during dynamic sparse training:

$$\mathbf{RI}_{ij} = \frac{|\mathbf{W}_{ij}|}{\sum |\mathbf{W}_{*j}|} + \frac{|\mathbf{W}_{ij}|}{\sum |\mathbf{W}_{i*}|} \quad (1)$$

As illustrated in Equation 1, RI assesses connections by normalizing the absolute weight of links that share the same input or output neurons. This method does not require calibration data and can perform comparably to the baseline post-training pruning methods like sparsegpt (Frantar & Alistarh, 2023) and wanda (Sun et al., 2023). Generally, WM and RI are straightforward, effective, and quick to implement in DST for link removal but give different directions for network percolation. WM prioritizes links with higher weight magnitudes, leading to rapid network percolation, whereas RI inherently values links connected to lower-degree nodes, thus maintaining a higher active neuron post-percolation (ANP) rate. The ANP rate is the ratio of the number of active neurons after training compared to the original number of neurons before training. These methods are equally valid but cater to different scenarios. For instance, using RI significantly improves results on the Fashion MNIST dataset compared to WM, whereas WM performs better on the MNIST and EMNIST datasets.

**Soft link removal.** In the early stages of training, both WM and RI are not reliable due to the model's underdevelopment. Therefore, rather than strictly selecting top values based on WM and RI, we also sample links from a multinomial distribution using an importance score calculated by the removal metrics. The final formula for link removal is defined in Equation 2.

$$\mathbf{S}_{ij} = \left( \frac{|\mathbf{W}_{ij}|/2}{\alpha + (1 - \alpha) \sum |\mathbf{W}_{i*}|} + \frac{|\mathbf{W}_{ij}|/2}{\alpha + (1 - \alpha) \sum |\mathbf{W}_{*j}|} \right)^{\frac{\delta}{1-\delta}} \quad (2)$$

Here,  $\alpha$  determines the removal strategy, shifting from weight magnitude ( $\alpha = 1$ ) to relative importance ( $\alpha = 0$ ). In all experiments, we only evaluate these two  $\alpha$  values.  $\delta$  adjusts the softness of the sampling process. As training progresses and weights become more reliable, we adaptively increase  $\delta$  from 0.5 to 0.75 to refine the sampling strategy and improve model performance. These settings are constant for all the experiments in this article.

**Node-based link regrowth.** Another significant challenge for CHT lies in the time complexity of link prediction. In the original CHT framework, the CH3-L3 metric is employed for link regrowth, defined as follows:

$$\mathbf{CH3-L3p}(u, v) = \sum_{z_1, z_2 \in L3} \frac{1}{\sqrt{de_{z_1}^* \cdot de_{z_2}^*}} \quad (3)$$

Here,  $u$  and  $v$  denote the seed nodes, while  $z_1$  and  $z_2$  are common neighbors on the L3 path (Muscoloni et al., 2022). The term  $de_i^*$  represents the number of external local community links (eLCL) of node  $i$ , with a default increment of 1 to prevent division by zero. Path-based link prediction has demonstrated its effectiveness on both real-world networks (Muscoloni et al., 2022) and artificial neural networks (Zhang et al., 2024b). However, this method incurs

a high computational cost due to the need to compute and store all length-three paths, resulting in a time complexity of  $O(N \cdot d^3)$ , where  $N$  is the number of nodes and  $d$  is the network’s average degree. This complexity is prohibitive for large models with numerous nodes and higher-density layers.

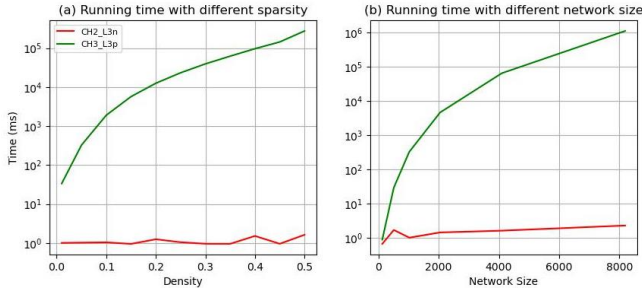


Figure 2: **Runtime Performance Evaluation** of node-based and path-based methods across varying densities and network sizes. In (a), the network size is fixed at  $1024 \times 1024$ , while in (b), the density is fixed at 5%.

To address this issue, we introduce a more efficient, node-based paradigm that eliminates the reliance on length-three paths between seed nodes. Instead, this approach focuses on the common neighbors of seed nodes. The node-based version of CH3-L3p, denoted as CH3-L3n, is defined as follows:

$$\text{CH3-L3n}(u, v) = \sum_{z \in L3} \frac{1}{de_z^*} \quad (4)$$

In addition to CH3-L3n, we propose a new node-based version of the CH theory, which also incorporates internal local community links (iLCL) to enhance the expressiveness of the formula. This variant, referred to as CH2-L3n, is formulated as:

$$\text{CH2-L3n}(u, v) = \sum_{z \in L3} \frac{di_z^*}{de_z^*} \quad (5)$$

We evaluate the runtime performance of both the path-based (CH3-L3p as represented) and node-based (CH2-L3n as represented) methods across varying network sizes and sparsity levels, as illustrated in Figure 2. The red and green lines depict the actual runtime for the path-based and node-based methods, respectively. The results reveal that the node-based version achieves significantly faster runtime performance compared to the path-based methods. Furthermore, the node-based method demonstrates consistently stable runtime across diverse network sizes and density levels, making it an ideal link prediction as the CH theory based link re-growth component of CHTs in dynamic sparse training for large-scale models.

### 3.2. Sparse Topological Initialization with Bipartite Small-World model

We introduce all the network science based sparse topological initialization methods in Section C. As demonstrated in CHT (Zhang et al., 2024b), the final trained model converges into an ultra-small-world network, exhibiting both scale-free and small-world properties. This raises a compelling question: what if the network is directly initialized with these characteristics? In this work, we investigate this by initializing networks with bipartite small-world (BSW) and bipartite scale-free (BSF) structures. To further enhance the performance of BSF initialization, we introduce two optimization techniques. However, as detailed in Appendix D, our findings indicate that networks initialized with the BSW structure consistently achieve superior performance.

The BSW model, with its small-world properties, ensures both high clustering and a short average path length. The high clustering, which is absent in the BSF model, increases the probability that seed nodes share common neighbors along L3 paths (paths of length three). This, in turn, improves the effectiveness of the CH-based link predictor in generating accurate predictions early in the training process. In contrast, the BSF model’s preferential attachment mechanism creates hub nodes and a sparsely clustered structure at initialization, which is randomly assigned. Early in training, this random hub assignment may not align with the actual training dynamics, while the highly power-law degree distribution can mislead the CH link predictor, causing it to stack within the ELM.

### 3.3. Sigmoid Gradual Decrease Density

As demonstrated in GraNet (Liu et al., 2021) and MEST<sub>EM&S</sub> (Yuan et al., 2021), incorporating a density decrease strategy can significantly improve the performance of dynamic sparse training. In MEST<sub>EM&S</sub>, the density is reduced discretely at predefined epochs. In GraNet, the network evolution process consists of three steps: pruning, link removal, and link regrowth. The method first prunes the network to reduce the density, followed by removing and regrowing an equivalent number of links under the updated density. The density decrease in GraNet follows the same approach as Gradual Magnitude Pruning (GMP) (Zhu & Gupta, 2017), which adheres to a cubic function:

$$s_t = s_f + (s_i - s_f) \left( 1 - \frac{t - t_0}{n\Delta t} \right)^3, \quad (6)$$

where  $t \in \{t_0, t_0 + \Delta t, \dots, t_0 + n\Delta t\}$ ,  $s_i$  is the initial sparsity,  $s_f$  is the target sparsity,  $t_0$  is the starting epoch of gradual pruning,  $t_f$  is the end epoch of gradual pruning, and  $\Delta t$  is the pruning frequency.

However, this density decay scheduler exhibits a sharp decline in the initial stages of training, which risks pruning a

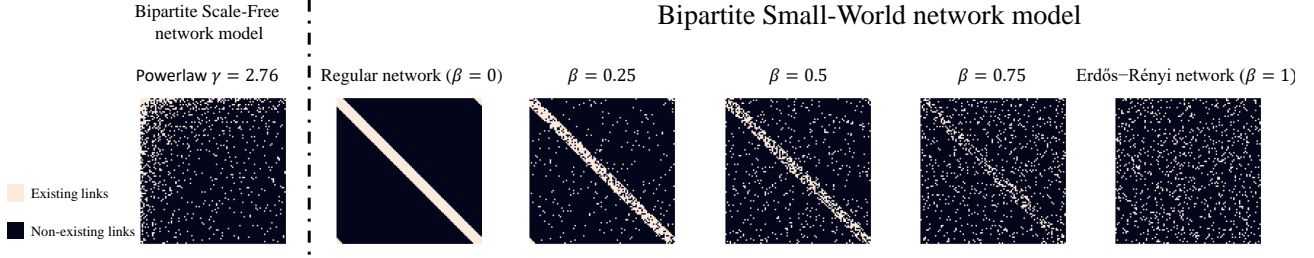


Figure 3: **The adjacency matrices** of the Bipartite Scale-Free (BSF) network model and the Bipartite Small-World (BSW) network model vary with different values of  $\beta$ . a) The BSF model inherently forms a scale-free network characterized by a power-law distribution with  $\gamma = 2.76$ . b) As  $\beta$  changes from 0 to 1, the network exhibits reduced clustering. It is important to note that when  $\beta = 0$ , the BSW model does not qualify as a small-world network.

substantial fraction of weights before the model has sufficiently learned. To mitigate this issue, we propose a sigmoid-based gradual density decrease strategy, defined as:

$$s_t = s_f + (s'_i - s_f) \left( \frac{1}{1 + e^{-k(t - \frac{t_f - t_0}{2})}} \right), \quad (7)$$

where  $k$  controls the curvature of the decrease. We set  $k=6$  for all the experiments in this article. This strategy ensures a smoother initial pruning phase, allowing the model to warm up and stabilize before undergoing significant pruning, thereby enhancing training stability and performance.

Since our work focuses on MLP, Transformer, and LLMs, where FLOPs are linearly related to the density of the linear layers, the FLOPs of the whole training process are linearly related to the integral of the density function across the training time. The integral of the GraNet decrease function from  $t_0$  to  $t_f$  is:

$$\int_{t_0}^{t_f} (s_i - s_f) \left( 1 - \frac{t - t_0}{n\Delta t} \right)^3 dt = \frac{1}{4}(s_i - s_f)(t_f - t_0). \quad (8)$$

For the sigmoid decrease, the integral is:

$$\int_{t_0}^{t'_f} (s'_i - s_f) \left( \frac{1}{1 + e^{-k(t - \frac{t'_f + t_0}{2})}} \right) dt = \frac{(s'_i - s_f)(t'_f - t_0)}{2}. \quad (9)$$

To maintain consistency in the computational cost (FLOPs) during training compared to the cubic decay strategy, we reduce the number of steps in the sigmoid-based gradual density decrease by half.

In addition to refining the decay function, we replace the weight magnitude criterion used in the original GMP and GraNet processes with relative importance (RI). This adjustment is motivated by prior work (Zhang et al., 2024a), which

has shown that RI provides a significant performance advantage over weight magnitude, particularly when pruning models initialized with high density.

## 4. Experiments

### 4.1. Experimental Setup

We evaluate the performance of CHTs using MLPs for image classification tasks on the MNIST (LeCun et al., 1998), Fashion MNIST (Xiao et al., 2017), and EMNIST (Cohen et al., 2017) datasets. To further validate our approach, we apply the sigmoid gradual density decay strategy to Transformers for machine translation tasks on the Multi30k en-de (Elliott et al., 2016), IWSLT14 en-de (Cettolo et al., 2014), and WMT17 en-de (Bojar et al., 2017) datasets. Additionally, we conduct language modeling experiments using the OpenWebText dataset (Gokaslan & Cohen, 2019) and evaluate zero-shot performance on the GLUE (Wang et al., 2019) and SuperGLUE (Wang et al., 2020) benchmark with LLaMA-130M (Touvron et al., 2023a). For MLP training, we sparsify all layers except the final layer, as ultra-sparsity in the output layer may lead to disconnected neurons, and the connections in the final layer are relatively minor compared to the previous layers. For Transformers and LLaMA-130M, we apply dynamic sparse training (DST) to all linear layers, excluding the embedding and final generator layer. Detailed hyperparameter settings for each experiment are provided in Tables 5, 6, and 7.

**Baseline Methods** We compare our method with the baseline approaches in the literature. We divide the dynamic sparse training (DST) methods into two categories: fixed sparsity DST and density decay DST. For the fixed sparsity DST, we compare CHTs with the SET (Mocanu et al., 2018), RigL (Evcı et al., 2020), and CHT (Zhang et al., 2024b) and for the density decay DST methods, we compare CHTs with MEST<sub>EM&S</sub> (Yuan et al., 2021), GMP (Zhu & Gupta, 2017), and GraNet (Liu et al., 2021). We explain the detailed implementations and the reason we split GMP as a type of DST method in Appendix F.

Table 1: Performance comparison of different fixed sparsity dynamic sparse training methods on MNIST, Fashion MNIST (FMNIST), and EMNIST datasets trained on MLP at 99% sparsity. ACC represents accuracy, and ANP denotes the active neuron percolation rate that indicates the final size of the network. The best method for each dataset is highlighted in bold and the performances better than the fully connected ones are marked with “\*”

Method	MNIST		FMNIST		EMNIST	
	ACC (%)	ANP (%)	ACC (%)	ANP (%)	ACC (%)	ANP (%)
FC	98.78 ± 0.02	-	90.88 ± 0.02	-	87.13 ± 0.04	-
CHTs (CH3-L3p)	<b>98.81 ± 0.04*</b>	20%	<b>90.93 ± 0.03*</b>	89%	87.61 ± 0.07*	24%
CHTs (CH2-L3n)	98.76 ± 0.05	27%	90.67 ± 0.05	73%	<b>87.82 ± 0.04*</b>	28%
CHT	98.48 ± 0.04	29%	88.70 ± 0.07	30%	86.35 ± 0.08	21%
RigL	98.61 ± 0.01	29%	89.91 ± 0.07	55%	86.94 ± 0.08	28%
SET	98.14 ± 0.02	100%	89.00 ± 0.09	100%	86.31 ± 0.08	100%

## 4.2. MLP for image classification

**Ablation Test.** Using MLP, we conduct an ablation study on each component proposed within the CHTs framework to determine the most effective implementation to apply next for the Transformer model. Figure 4a) compares the topologies initialized with the Bipartite Small-World (BSW) model at different values of  $\beta$ , clearly indicating that  $\beta = 0.25$  yields the best results. Figures 4b) assess the link removal methods, concluding that the weight magnitude soft (WM-soft) method outperforms all others. We consider the best settings showcased in these results to decide the CHTs strategy for training Transformers and LLaMA-130M.

**Main Results.** In the MLP evaluation, we aim to assess the fundamental capacity of DST methods to train the fully connected module, which is common across many ANNs. The sparse topological initialization of CHTs is CSTI since the input bipartite layer can directly receive information from the input pixels. Table 1 displays the performance of DST methods compared to their fully connected counterparts across three basic datasets. The DST methods are tested at 99% sparsity. As shown in Table 1, both of the two regrowth methods of CHTs outperform the other fixed sparsity DST methods. Notably, the path-based CH3-L3p outperforms the fully connected one in all the datasets. The node-based CH2-L3n also achieves comparable performance on these basic datasets. In addition, we present the active neuron post-percolation rate (ANP) for each method in Table 1. It is evident that CHTs adaptively percolates the network more effectively while retaining performance.

## 4.3. Transformer on Machine Translation

We assess the Transformer’s performance on a classic machine translation task across three datasets. We take the best performance of the model on the validation set and report the BLEU on the test set. Beam search, with a beam size of 2, is employed to optimize the evaluation process. In our evaluation, CHTs configures the topology of each layer using the BSW model with  $\beta = 0.25$ , employs WM-soft for

link removal, and regrows new links using CH2-L3n-soft. Additionally, we apply an adjusted network percolation technique to the Transformer, as detailed in Appendix Section E. The findings, presented in Table 2, demonstrate that 1) CHTs surpasses other fixed density DST methods on all the sparsity scenarios. 2) Incorporating with the sigmoid density decrease, CHTs outperforms even the fully connected ones with only 5% density.

## 4.4. Natural Language Generation

**Language modeling.** We utilize LLaMA-130M (Touvron et al., 2023a) architecture as the baseline for our language generation experiments. For LLaMA, we follow the experiment setup from (Zhao et al., 2024) and detailed in Table 7. To ensure the FLOPs are the same for all the density decrease methods, for CHTs, we implement a half-step strategy for the density decay steps.

As shown in Table 3, we show the validation perplexity results of each algorithm across the density decrease. As shown, CHTs stably outperformance SET and RigL while CHTs constantly better than GraNet and GMP. At 70% sparsity, CHTs is already able to perform a comparable performance in comparison to the fully connected. It is important to note that RigL and GraNet exhibit subpar performance in this evaluation due to the use of bfloat16 precision in this configuration. This lower precision adversely impacts gradient accuracy, particularly in the early stages of training. Since both RigL and GraNet rely on gradient information to regrow new links, the imprecise gradients lead to regrowing wrong links, thereby hindering their performance.

**Zero-shot evaluations.** The pretrained model of CHTs with 30% sparsity and the fully connected one are evaluated the zero-shot performance on the GLUE (Wang et al., 2019)(cola, sst2, mrpc, qqp, mnli, qnli, rte, wnli) and SuperGLUE (Wang et al., 2020) (boolq, hellaswag, CB, copa). We show the results in Table 4. The performance difference between FC and CHTs is statistically significant (p-value =

Table 2: Performance comparison on machine translation tasks of Multi30k, IWSLT, and WMT with varying sparsity levels. The scores indicate BLEU scores, which is the higher the better. CHTs (GMP) indicates CHTs uses GMP’s density decay strategy. The best performance on each dataset is highlighted in bold and the performances better than the fully connected ones are marked with “\*”.  $s_i$  indicates the starting sparsity of the dst methods that use density decay strategy.

Method	Multi30k		IWSLT		WMT	
	95%	90%	95%	90%	95%	90%
FC	31.28		24.2		25.22	
SET	27.89	28.72	18.48	19.54	20.21	21.61
RigL	27.63	28.89	20.29	21.03	20.52	22.16
CHTs	28.12	30.35	20.55	21.60	21.14	22.68
MEST <sub>EM&amp;S</sub>	28.71	28.26	18.95	20.77	20.79	22.3
GMP ( $s_i = 0.5$ )	26.42	27.06	22.44	22.62	22.29	23.52
GraNet ( $s_i = 0.5$ )	30.90	31.06	23.05	22.88	22.11	23.49
CHTs (GMP) ( $s_i = 0.5$ )	30.49	30.33	23.68	23.64	<b>22.8</b>	23.22
<b>CHTss</b> ( $s_i = 0.5$ )	<b>32.04*</b>	<b>32.79*</b>	<b>24.86*</b>	<b>24.57*</b>	22.68	<b>24.05</b>

Table 3: **Validation perplexity of different dynamic sparse training (DST) methods on OpenWebText using LLaMA-130M across varying sparsity levels.** Bold values denote the best performance among DST methods. Lower perplexity corresponds to better model performance.  $s_i$  represents the initial sparsity for DST methods employing a density decay strategy.

Method	Sparsity			
	95%	90%	80%	70%
FC	19.27			
SET	28.37	24.73	22.02	20.82
RigL	49.39	37.18	66.35	25.85
CHTs	27.72	24.24	21.70	21.15
MEST <sub>EM&amp;S</sub>	27.96	24.98	22.21	21.32
GMP ( $s_i = 0.5$ )	27.16	23.61	22.28	20.49
GraNet ( $s_i = 0.5$ )	61.31	26.81	29.03	22.84
CHTs (GMP) ( $s_i = 0.5$ )	26.81	22.94	20.94	20.01
<b>CHTss</b> ( $s_i = 0.5$ )	<b>25.29</b>	<b>22.71</b>	<b>20.78</b>	<b>19.92</b>

0.01) according to a paired two-sided Wilcoxon signed rank test, which means CHTss is significantly better than fully connected ones in zero-shot evaluations.

## 5. Conclusion and Discussion

We move forward the current knowledge in brain-inspired dynamic sparse training, proposing the Cannistraci-Hebb Training soft rule with sigmoid gradual density decay (CHTss). First, we introduce a matrix multiplication mathematical formula for GPU-friendly approximation of the CH link predictor. This significantly reduces the computational complexity of CHT and speeds up the running time, enabling the implementation of CHT in large-scale models. Second, we propose a Cannistraci-Hebb training soft rule (CHTs), which innovatively utilizes a soft sampling rule for both removal and regrowth links striking a balance

Table 4: Zero-shot evaluation of LLaMA-130M between fully connected pretrained and pretrained with CHTss (70% sparsity) across GLUE and Superglue datasets. MRPC and QQP use F1 scores while the others use ACC.  $s_i$  indicates the starting sparsity of the dst methods that use density decay strategy.

Dataset	FC	CHTss ( $s_i = 0.5$ )
CoLA	65.29 ± 1.47	<b>69.13 ± 1.43</b>
MNLI	32.44 ± 0.47	<b>32.72 ± 0.47</b>
MRPC	64.96 ± 2.36	<b>81.05 ± 1.64</b>
QNLI	<b>50.38 ± 0.68</b>	49.37 ± 0.68
QQP	52.09 ± 0.28	<b>53.82 ± 0.26</b>
RTE	48.38 ± 3.01	<b>50.54 ± 3.01</b>
SST-2	<b>49.54 ± 1.69</b>	49.08 ± 1.69
WNLI	49.30 ± 5.98	<b>52.11 ± 5.97</b>
Hellaswag	26.95 ± 0.44	<b>26.97 ± 0.44</b>
Boolq	43.85 ± 0.87	<b>56.79 ± 0.87</b>
CB	46.43 ± 6.72	<b>50.00 ± 6.74</b>
Copa	56.00 ± 4.99	<b>57.00 ± 4.98</b>
AVG	48.80	<b>52.38</b>
Win rate	0.17	<b>0.83</b>

for topological exploration and exploitation. Third, in transformer-based models, we integrate CHTs with a sigmoid gradual density decay strategy (CHTss). Empirically, CHTs demonstrate a remarkable ability to achieve ultra-sparse configurations—up to 99% sparsity in MLPs for image classification—surpassing fully connected networks. Notably, the regrowth process under CHTs does not rely on gradients. In contrast to RigL, which depends on inputs, topology, weights, and activation functions for predicting new connections, CHTs’ regrowth is merely brain-inspired and network topology-driven. With the sigmoid gradual density decay, CHTss surpasses the fully connected Transformer using only 5% density and achieves comparable language modeling performance, along with better zero-shot results, to the fully connected LLaMA-130M at just

30% density. This represents a relevant result for dynamic sparse training. We describe the limitations of this study and future works in [Appendix A](#).

## Impact Statement

This paper presents work whose goal is to advance the field of Machine Learning. There are many potential societal consequences of our work, none which we feel must be specifically highlighted here.

## References

- Barabási, A.-L. and Albert, R. Emergence of scaling in random networks. *science*, 286(5439):509–512, 1999.
- Bellec, G., Kappel, D., Maass, W., and Legenstein, R. Deep rewiring: Training very sparse deep networks. *arXiv preprint arXiv:1711.05136*, 2017.
- Bojar, O., Chatterjee, R., Federmann, C., Graham, Y., Haddow, B., Huang, S., Huck, M., Koehn, P., Liu, Q., Logacheva, V., et al. Findings of the 2017 conference on machine translation (wmt17). Association for Computational Linguistics, 2017.
- Cannistraci, C. V. Modelling self-organization in complex networks via a brain-inspired network automata theory improves link reliability in protein interactomes. *Sci Rep*, 8(1):2045–2322, 10 2018. doi: 10.1038/s41598-018-33576-8.
- Cannistraci, C. V., Alanis-Lobato, G., and Ravasi, T. From link-prediction in brain connectomes and protein interactomes to the local-community-paradigm in complex networks. *Scientific reports*, 3(1):1613, 2013.
- Cettolo, M., Niehues, J., Stüker, S., Bentivogli, L., and Federico, M. Report on the 11th IWSLT evaluation campaign. In Federico, M., Stüker, S., and Yvon, F. (eds.), *Proceedings of the 11th International Workshop on Spoken Language Translation: Evaluation Campaign*, pp. 2–17, Lake Tahoe, California, December 4-5 2014. URL <https://aclanthology.org/2014.iwslt-evaluation.1>.
- Cohen, G., Afshar, S., Tapson, J., and Van Schaik, A. Emnist: Extending mnist to handwritten letters. In *2017 international joint conference on neural networks (IJCNN)*, pp. 2921–2926. IEEE, 2017.
- Daminelli, S., Thomas, J. M., Durán, C., and Cannistraci, C. V. Common neighbours and the local-community-paradigm for topological link prediction in bipartite networks. *New Journal of Physics*, 17(11):113037, nov 2015. doi: 10.1088/1367-2630/17/11/113037. URL <https://doi.org/10.1088/1367-2630/17/11/113037>.
- Dao, T., Chen, B., Sohoni, N. S., Desai, A., Poli, M., Grogan, J., Liu, A., Rao, A., Rudra, A., and Ré, C. Monarch: Expressive structured matrices for efficient and accurate training. In *International Conference on Machine Learning*, pp. 4690–4721. PMLR, 2022.
- Drachman, D. A. Do we have brain to spare?, 2005.
- Durán, C., Daminelli, S., Thomas, J. M., Haupt, V. J., Schroeder, M., and Cannistraci, C. V. Pioneering topological methods for network-based drug–target prediction by exploiting a brain-network self-organization theory. *Briefings in Bioinformatics*, 19(6):1183–1202, 04 2017. doi: 10.1093/bib/bbx041. URL <https://doi.org/10.1093/bib/bbx041>.
- Elliott, D., Frank, S., Sima’an, K., and Specia, L. Multi30k: Multilingual english-german image descriptions. In *Proceedings of the 5th Workshop on Vision and Language*, pp. 70–74. Association for Computational Linguistics, 2016. doi: 10.18653/v1/W16-3210. URL <http://www.aclweb.org/anthology/W16-3210>.
- ERDdS, P. and R&wi, A. On random graphs i. *Publ. math. debrecen*, 6(290-297):18, 1959.
- Evcı, U., Gale, T., Menick, J., Castro, P. S., and Elsen, E. Rigging the lottery: Making all tickets winners. In *Proceedings of the 37th International Conference on Machine Learning, ICML 2020, 13-18 July 2020, Virtual Event*, volume 119 of *Proceedings of Machine Learning Research*, pp. 2943–2952. PMLR, 2020. URL <http://proceedings.mlr.press/v119/evci20a.html>.
- Frantar, E. and Alistarh, D. Massive language models can be accurately pruned in one-shot. *arXiv preprint arXiv:2301.00774*, 2023.
- Gokaslan, A. and Cohen, V. Openwebtext corpus. <http://Skyllion007.github.io/OpenWebTextCorpus>, 2019.
- Han, S., Pool, J., Tran, J., and Dally, W. Learning both weights and connections for efficient neural network. *Advances in neural information processing systems*, 28, 2015.
- Han, S., Mao, H., and Dally, W. J. Deep compression: Compressing deep neural network with pruning, trained quantization and huffman coding. In Bengio, Y. and LeCun, Y. (eds.), *4th International Conference on Learning Representations, ICLR 2016, San Juan, Puerto Rico, May 2-4, 2016, Conference Track Proceedings*, 2016. URL <http://arxiv.org/abs/1510.00149>.
- Hebb, D. The organization of behavior. emphnew york, 1949.

- Jayakumar, S., Pascanu, R., Rae, J., Osindero, S., and Elsen, E. Top-kast: Top-k always sparse training. *Advances in Neural Information Processing Systems*, 33:20744–20754, 2020.
- Lasby, M., Golubeva, A., Evci, U., Nica, M., and Ioannou, Y. Dynamic sparse training with structured sparsity. *arXiv preprint arXiv:2305.02299*, 2023.
- LeCun, Y., Bottou, L., Bengio, Y., and Haffner, P. Gradient-based learning applied to document recognition. *Proc. IEEE*, 86(11):2278–2324, 1998. doi: 10.1109/5.726791. URL <https://doi.org/10.1109/5.726791>.
- Lee, N., Ajanthan, T., and Torr, P. H. S. Snip: single-shot network pruning based on connection sensitivity. In *7th International Conference on Learning Representations, ICLR 2019, New Orleans, LA, USA, May 6-9, 2019*. OpenReview.net, 2019. URL <https://openreview.net/forum?id=B1VZqjAcYX>.
- Li, M., Liu, R.-R., Lü, L., Hu, M.-B., Xu, S., and Zhang, Y.-C. Percolation on complex networks: Theory and application. *Physics Reports*, 907:1–68, 2021.
- Liu, S., Chen, T., Chen, X., Atashgahi, Z., Yin, L., Kou, H., Shen, L., Pechenizkiy, M., Wang, Z., and Mocanu, D. C. Sparse training via boosting pruning plasticity with neuroregeneration. *Advances in Neural Information Processing Systems*, 34:9908–9922, 2021.
- Mocanu, D. C., Mocanu, E., Stone, P., Nguyen, P. H., Gibescu, M., and Liotta, A. Scalable training of artificial neural networks with adaptive sparse connectivity inspired by network science. *Nature communications*, 9(1):1–12, 2018.
- Muscoloni, A., Michieli, U., Zhang, Y., and Cannistraci, C. V. Adaptive network automata modelling of complex networks. *Preprints*, May 2022. doi: 10.20944/preprints202012.0808.v3. URL <https://doi.org/10.20944/preprints202012.0808.v3>.
- Narula, V. e. a. Can local-community-paradigm and epitopological learning enhance our understanding of how local brain connectivity is able to process, learn and memorize chronic pain? *Applied network science*, 2(1), 2017. doi: 10.1007/s41109-017-0048-x.
- Prabhu, A., Varma, G., and Nambodiri, A. Deep expander networks: Efficient deep networks from graph theory. In *Proceedings of the European Conference on Computer Vision (ECCV)*, pp. 20–35, 2018.
- Stewart, J., Michieli, U., and Ozay, M. Data-free model pruning at initialization via expanders. In *Proceedings of the IEEE/CVF Conference on Computer Vision and Pattern Recognition*, pp. 4518–4523, 2023.
- Sun, M., Liu, Z., Bair, A., and Kolter, J. Z. A simple and effective pruning approach for large language models. *arXiv preprint arXiv:2306.11695*, 2023.
- Thangarasa, V., Gupta, A., Marshall, W., Li, T., Leong, K., DeCoste, D., Lie, S., and Saxena, S. Spdf: Sparse pre-training and dense fine-tuning for large language models. In *Uncertainty in Artificial Intelligence*, pp. 2134–2146. PMLR, 2023.
- Touvron, H., Lavril, T., Izacard, G., Martinet, X., Lachaux, M.-A., Lacroix, T., Rozière, B., Goyal, N., Hambro, E., Azhar, F., et al. Llama: Open and efficient foundation language models. *arXiv preprint arXiv:2302.13971*, 2023a.
- Touvron, H., Martin, L., Stone, K., Albert, P., Almahairi, A., Babaei, Y., Bashlykov, N., Batra, S., Bhargava, P., Bhosale, S., et al. Llama 2: Open foundation and fine-tuned chat models. *arXiv preprint arXiv:2307.09288*, 2023b.
- Vaswani, A., Shazeer, N., Parmar, N., Uszkoreit, J., Jones, L., Gomez, A. N., Kaiser, Ł., and Polosukhin, I. Attention is all you need. *Advances in neural information processing systems*, 30, 2017.
- Walsh, C. A. Peter huttenlocher (1931–2013). *Nature*, 502(7470):172–172, 2013.
- Wang, A., Singh, A., Michael, J., Hill, F., Levy, O., and Bowman, S. R. Glue: A multi-task benchmark and analysis platform for natural language understanding, 2019. URL <https://arxiv.org/abs/1804.07461>.
- Wang, A., Pruksachatkun, Y., Nangia, N., Singh, A., Michael, J., Hill, F., Levy, O., and Bowman, S. R. Superglue: A stickier benchmark for general-purpose language understanding systems, 2020. URL <https://arxiv.org/abs/1905.00537>.
- Watts, D. J. and Strogatz, S. H. Collective dynamics of ‘small-world’ networks. *nature*, 393(6684):440–442, 1998.
- Xiao, H., Rasul, K., and Vollgraf, R. Fashion-mnist: a novel image dataset for benchmarking machine learning algorithms. *arXiv preprint arXiv:1708.07747*, 2017.
- Yuan, G., Ma, X., Niu, W., Li, Z., Kong, Z., Liu, N., Gong, Y., Zhan, Z., He, C., Jin, Q., et al. Mest: Accurate and fast memory-economic sparse training framework on the edge. *Advances in Neural Information Processing Systems*, 34: 20838–20850, 2021.
- Zhang, S., Roller, S., Goyal, N., Artetxe, M., Chen, M., Chen, S., Dewan, C., Diab, M., Li, X., Lin, X. V., et al. Opt: Open pre-trained transformer language models. *arXiv preprint arXiv:2205.01068*, 2022.

Zhang, Y., Bai, H., Lin, H., Zhao, J., Hou, L., and Cannistraci, C. V. Plug-and-play: An efficient post-training pruning method for large language models. In *The Twelfth International Conference on Learning Representations*, 2024a. URL <https://openreview.net/forum?id=Tr0lPx9woF>.

Zhang, Y., Zhao, J., Wu, W., Muscoloni, A., and Cannistraci, C. V. Epi-topological learning and cannistraci-hebb network shape intelligence brain-inspired theory for ultra-sparse advantage in deep learning. In *The Twelfth International Conference on Learning Representations*, 2024b. URL <https://openreview.net/forum?id=iayEcORsGd>.

Zhao, J., Zhang, Z., Chen, B., Wang, Z., Anandkumar, A., and Tian, Y. Galore: Memory-efficient llm training by gradient low-rank projection, 2024. URL <https://arxiv.org/abs/2403.03507>.

Zhu, M. and Gupta, S. To prune, or not to prune: exploring the efficacy of pruning for model compression, 2017. URL <https://arxiv.org/abs/1710.01878>.

Table 5: Hyperparameters of MLP on Image Classification Tasks.

Hyper-parameter	MLP
Hidden Dimension	1568
# Hidden layers	3
Batch Size	32
Training Epochs	100
LR Decay Method	Linear
Learning Rate	0.025
$\zeta$ (fraction of removal)	0.3
Update Interval (for DST)	1

Table 6: Hyperparameters of Transformer on Machine Translation Tasks.

Hyper-parameter	Multi30k	IWSLT14	WMT17
Embedding Dimension	512	512	512
Feed-forward Dimension	1024	2048	2048
Batch Size	1024 tokens	10240 tokens	12000 tokens
Training Steps	5000	20000	80000
Dropout	0.1	0.1	0.1
Attention Dropout	0.1	0.1	0.1
Max Gradient Norm	0	0	0
Warmup Steps	1000	6000	8000
Decay Method	inoam	inoam	inoam
Label Smoothing	0.1	0.1	0.1
Layer Number	6	6	6
Head Number	8	8	8
Learning Rate	0.25	2	2
$\zeta$ (fraction of removal)	0.3	0.3	0.3
Update Interval (for DST)	100	100	100

## A. Limitation

A potential limitation of this work is that the hardware required to accelerate sparse training with unstructured sparsity has not yet become widely adopted. Consequently, this article does not present a direct comparison of training speeds with those of fully connected networks. However, several leading companies (Thangarasa et al., 2023) have already released devices that support unstructured sparsity in training.

For future work, we aim to develop methods for automatically determining the temperature for soft sampling at each epoch, guided by the topological features of each layer. This could enable each layer to learn its specific topological rules autonomously. Additionally, we plan to test CHTs in larger LLMs such as LLaMA-1b and LLaMA-7b to evaluate the performance in scenarios with denser layers.

## B. Broader Impact

In this work, we introduce a novel methodology for dynamic sparse training aimed at enhancing the efficiency of AI model training. This advancement holds potential societal benefits by increasing interest in more efficient AI practices. However, the widespread availability of advanced artificial neural networks, particularly large language models (LLMs), also presents risks of misuse. It is essential to carefully consider and manage these factors to maximize benefits and minimize risks.

Table 7: **Hyperparameters of LLaMA-130M on OpenWebText.**

Hyper-parameter	LLaMA-130M
Embedding Dimension	768
Feed-forward Dimension	2048
Global Batch Size	512
Sequence Length	256
Training Steps	30000
Learning Rate	3e-3
Warmup Steps	10000
Optimizer	Adam
Layer Number	12
Head Number	12
$\zeta$ (fraction of removal)	0.1
Update Interval (for DST)	100

### C. Sparse topological initialization

**Correlated sparse topological initialization.** Correlated Sparse Topological Initialization (CSTI) is a physical-informed topological initialization. CSTI generates the adjacency matrix by computing the Pearson correlation between each input feature across the calibration dataset and then selects the predetermined number of links, calculated based on the desired sparsity level, as the existing connections. CSTI performs remarkably better when the layer can directly receive input information. However, for layers that cannot receive inputs directly, it cannot capture the correlations from the start since the model is initialized randomly, as in the case of the Transformer. Therefore, in this article, we aim to address this issue by investigating different network models to initialize the topology, with the goal of improving the performance for cases where CSTI cannot be directly applied.

**Bipartite scale-free model.** In artificial neural networks (ANNs), fully connected networks are inherently bipartite. This article explores initializing bipartite networks using models from network science. The Bipartite Scale-Free (BSF) (Zhang et al., 2024b) network model extends the concept of scale-freeness to bipartite structures, making them suitable for dynamic sparse training. Initially, the BSF model generates a monopartite Barabási-Albert (BA) model (Barabási & Albert, 1999), a well-established method for creating scale-free networks in which the degree distribution follows a power law ( $\gamma=2.76$  in Figure 3). Following the creation of the BA model, the BSF approach removes any connections between nodes of the same type (neuron in the same layer) and rewires these connections to nodes of the opposite type (neuron in the opposite layer). This rewiring is done while maintaining the degree of each node constant to preserve the power-law exponent  $\gamma$ .

**Bipartite small-world model.** The Bipartite Small-World (BSW) network model (Zhang et al., 2024b) is designed to incorporate small-world properties and high clustering coefficient into bipartite networks. Initially, the model constructs a regular ring lattice and assigns two distinct types of nodes to it. Each node is connected by an equal number of links to the nearest nodes of the opposite type, fostering high clustering but lacking the small-world property. Similar to the Watts-Strogatz model (WS) (Watts & Strogatz, 1998), the BSW model introduces a rewiring parameter,  $\beta$ , which represents the percentage of links randomly removed and then rewired within the network. At  $\beta = 1$ , the model transitions into an **Erdős-Rényi model** (ERDdS & R&wi, 1959), exhibiting small-world properties but without high clustering coefficient, which is popular as the topological initialization of the other dynamic sparse training methods (Mocanu et al., 2018; Evci et al., 2020; Yuan et al., 2021).

### D. Equal Partition and Neuron Resorting to enhance bipartite scale-free network initialization

As indicated in SET and CHT (Mocanu et al., 2018; Zhang et al., 2024b), trained sparse models typically converge to a scale-free network. This suggests that initiating the network with a scale-free structure might initially enhance performance. However, starting directly with a Bipartite Scale-Free model (BSF, power-law exponent  $\gamma = 2.76$ ) does not yield effective results. Upon deeper examination, two potential reasons emerge:

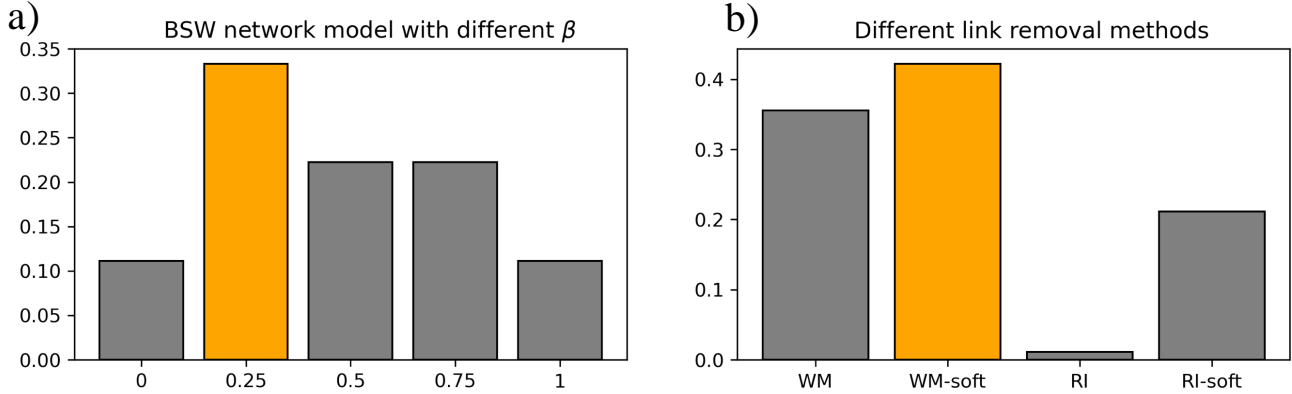


Figure 4: **The ablation test** of the  $\beta$  of the bipartite small world model and the removal methods in CHTs. a) evaluates the influence of the rewiring rate  $\beta$  on the model performance when initialized with the Bipartite Small-World network model (BSW). b) assess the influence of link removal selecting from the weight magnitude (WM), weight magnitude soft (WM-soft), relative importance (RI), and relative importance soft (RI-soft). We utilize the win rate of the compared factors under the same setting across each realization of 3 seeds for all experiment combinations on MLP. The factor with the highest win rate is highlighted in orange.

- The BSF model generates hub nodes randomly. However, This random assignment of hub nodes to less significant inputs leads to a less effective initialization, which is particularly detrimental in CHT, which merely utilizes the topology information to regrow new links.
- As demonstrated in CHT, in the final network, the hub nodes of one layer’s output should correspond to the input layer of the subsequent layer, which means the hub nodes should have a high degree on both sides of the layer. However, the BSF model’s random selection disrupts this correspondence, significantly reducing the number of Credit Assignment Paths (CAP) (Zhang et al., 2024b) in the model. CAP is defined as the chain of the transformation from input to output, which counts the number of links that go through the hub nodes in the middle layers.

To address these issues, we propose two solutions:

- **Equal Partitioning of the First Layer:** We begin by generating a BSF model, then rewire the connections from the input layer to the first hidden layer. While keeping the out-degrees of the output neurons fixed, we randomly sample new connections to the input neurons until each of the input neurons’ in-degrees reaches the input layer’s average in-degree. This approach ensures all input neurons are assigned equal importance while maintaining the power-law degree distribution of output neurons.
- **Resorting Middle Layer Neurons:** Given the mismatch in hub nodes between consecutive layers, we suggest permuting the neurons between the output of one layer and the input of the next, based on their degree. A higher degree in an output neuron increases the likelihood of connecting to a high-degree input neuron in the subsequent layer, thus enhancing the number of CAPs.

As illustrated in Figure 5, while the two techniques enhance the performance of the BSF initialization, they remain inferior to the BSW initialization. As noted in the main text, achieving scale-freeness is more effective when the model is allowed to learn and adapt dynamically rather than being directly initialized as a predefined structure.

## E. Network percolation and extension to Transformer.

We have adapted network percolation (Li et al., 2021; Zhang et al., 2024b) to suit the architecture of the Transformer after link removal. The underlying concept involves identifying inactive neurons, which we define as those lacking connections on one or both sides of a neuron layer. Such neurons disrupt the flow of information during forward propagation or backpropagation. In addition, Layer-wise computation of the CH link prediction score further implies that neurons without

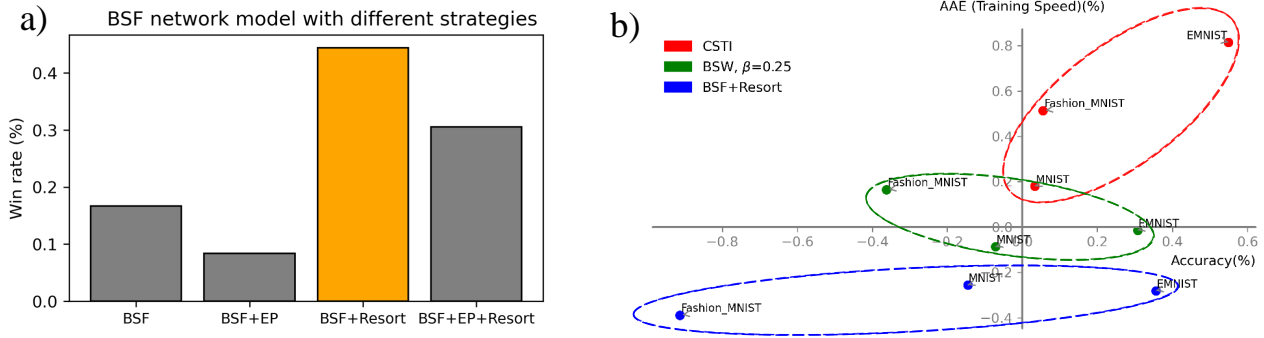


Figure 5: **The Performance** of the bipartite scale-free model and two enhanced techniques. a) shows the win rate of the Bipartite Scale-Free network model (BSF) with the different techniques. *EP* stands for equal partition of the first layer, and *Resort* refers to reordering the neurons based on their degree. b) assesses the comparison between Correlated Sparse Topological Initialization (CSTI), the Bipartite Scale-Free (BSF) model with the best solution from a), and the Bipartite Small-World (BSW) model with  $\beta = 0.25$ .

connections on one side are unlikely to form connections in the future. Therefore, network percolation becomes essential to optimize the use of remaining links.

As shown in Figure 1, network percolation encompasses two primary processes: c1) inactive neuron removal to remove the neurons that lack connections on one or both sides; c2) incomplete path adjustment to remove the incomplete paths where links connect to the inactive neurons after c1). Typically applied in simpler continuous layers like those in an MLP, network percolation requires modification for more complex structures. For example, within the Transformer’s self-attention module, the outputs of the query and key layers undergo a dot product operation. It necessitates percolation in these layers to examine the activity of the neurons in both output layers at the same position. Similar interventions are necessary in the `up_proj` and `gate_proj` layers of the MLP module in the LLaMA model family (Touvron et al., 2023a;b).

## F. Baseline Methods

### F.1. Fixed Density Dynamic Sparse Training Methods

**SET** (Mocanu et al., 2018): Removes connections based on weight magnitude and randomly regrows new links.

**RigL** (Evci et al., 2020): Removes connections based on weight magnitude and regrows links using gradient information, gradually reducing the proportion of updated connections over time.

**CHT** (Zhang et al., 2024b): A state-of-the-art (SOTA) gradient-free method that removes links with weight magnitude and regrows links based on CH3-L3 scores. (Note: CHT is only evaluated on MLPs due to its computational cost in large models.)

### F.2. Gradual Density Decrease Dynamic Sparse Training Methods

**GMP** (Han et al., 2015; Zhu & Gupta, 2017): Prunes the network with weight magnitude and gradually decrease the density based on Equation 8. Although originally a pruning method, GMP is treated as a dynamic sparse training method in their implementation (Zhu & Gupta, 2017), as it stores historical weights and allows pruned weights to reappear during training since, during training, the pruning threshold might change.

**MEST<sub>EM&S</sub>** (Yuan et al., 2021): Implements a two-stage density decrease strategy as described in the original work. It removes links based on the combination of weight magnitude and  $0.01 * \text{gradient}$  and regrows new links randomly.

**GraNet** (Liu et al., 2021): Gradually decreases density using Equation 8. Similar to RigL, GraNet removes links based on the weight magnitude and regrows new links with the gradient of the existing links.